Heliyon 10 (2024) e38540

Contents lists available at ScienceDirect

Heliyon

journal homepage: www.cell.com/heliyon

Research article

Optimal control and cost-effectiveness analysis of Fasciola hepatica model

Dagnaw Tantie Yihunie [a,*], Joseph Y.T. Mugisha [b], Dawit Melese Gebru [c], Haileyesus Tessema Alemneh [d]

[a] Department of Mathematics, Bahir Dar University, Debre Tabor University, Ethiopia
[b] Department of Mathematics, Makerere University, P.O. Box 7062, Kampala, Uganda
[c] Department of Mathematics, Bahir Dar University, P.O. Box 79, Bahir Dar, Ethiopia
[d] Department of Mathematics, University of Gondar, P.O. Box 196, Gondar, Ethiopia

ARTICLE INFO

Keywords:
Optimal control
Volterra–Lyapunov stability
Global stability
Pontryagin maximum principle
Cost-effectiveness

ABSTRACT

A deterministic model with an optimal control framework is formulated to analyse the cost-effectiveness of intervention measures used to control Fasciola hepatica in cattle populations. Using the Volterra-Lyapunov stability method, it is noted that the model is globally stable at the endemic equilibrium point. The Pontryagin maximum principle has been applied to determine optimal disease control conditions, including strategies such as pasture management, treatment of infected cattle, and molluscicide use. Numerical simulations for the optimum problem show that double and triple controls have significant effects on reducing disease transmission. The results indicate that for optimal impact, the molluscicide control parameter should always be at its highest possible value. The incremental cost-effectiveness ratio (ICER) analysis of strategies to reduce the disease shows that pasture management combined with molluscicide use will be the most effective and least expensive option. The molluscicide intervention rate should always be at its maximum value for better control of the disease. Educational programs for proper pasture management conditions and sufficient use of molluscicides can significantly reduce the spread of Fasciola hepatica among cattle and humans.

1. Introduction

Fascioliasis infections are caused by parasitic flatworms known as liver flukes, specifically, Fasciola hepatica and Fasciola gigantic [1–4]. These parasites primarily assault the liver of a wide variety of animals, particularly domesticated cattle, sheep, goats, and other ruminants. It is a worldwide disease except in places like Antarctica. However, it often hits very high prevalence in certain wet and marshy areas due to the fact that such conditions favour the survival of these parasites [5–7]. While Fasciola hepatica prevails in temperate regions of Europe, the Americas, and Oceania, it usually infects cattle and sheep, although it may occur in other domestic and wild mammals [8,9].

Fasciola hepatica is a foodborne zoonosis transmitted via contaminated water and food; its presence requires that the lymnaeid snails as intermediate hosts for the development [2,10]. The infection is caused by ingestion of the metacercaria stage of the parasite.

* Corresponding author.
E-mail addresses: dagntan@dtu.edu.et (D.T. Yihunie), joseph.mugisha@mak.ac.ug (J.Y.T. Mugisha), dawit.melese@bdu.edu.et (D.M. Gebru), haileyesus.tessema@uog.edu.et (H.T. Alemneh).

https://doi.org/10.1016/j.heliyon.2024.e38540
Received 11 March 2024; Received in revised form 23 September 2024; Accepted 25 September 2024

Available online 1 October 2024

It has a complex life cycle involving snails and mammals, which causes extensive damage to the liver, and the symptoms include hepatomegaly, abdominal pain, high fever, anaemia, jaundice, and loss of body weight. They can eventually lead to hepatic failure [6]. The life cycle of the liver fluke involves freshwater snails of the genera Galba and Lymnaea as intermediate hosts. Eggs excreted by adult flukes in mammalian hosts contaminate the water bodies and hatch into miracidia larvae. The larvae penetrate certain snails and follow several developmental stages [11]. After leaving the snails, they become infective metacercariae, which grazing animals ingest through contaminated water or vegetation [12]. The clinical signs and incubation period vary among host species in several factors [13]. However, the incubation period for fascioliasis in humans and cattle usually ranges $2-4$ months [11].

Differential diagnoses for bovine fascioliasis include clinical signs, grazing history and seasonal patterns, faecal analysis, post-mortem examinations and detection of the flukes in the liver [14,15]. Diagnosis by these methods is entirely accurate, hence the selection of appropriate treatment and control measures to lower the disease's impact on the concerned livestock. Avoidance of contaminated water and plants or parts thereof, deworming, management of pastures, snail control, and sanitation are all measures for prevention. The drug of choice for treatment is triclabendazole, but there is no vaccine against this disease [16]. Intermediate host populations must be reduced or treated with anthelmintics for effective control [15,17].

Fasciola hepatica is increasingly becoming a significant concern to animal and public health, having enormous economic and medical impacts. Globally, it affects 600-700 million animals and threatens 180 million people [18], an estimated cost of over $3.2 billion annually in the lost productivity of animals [19]. The disease reduces milk and meat production by 8% to 80% [20,21]. Such effective control, early detection, and treatment are essential. Modelling is critical to understanding and managing its spread; various models were developed to simulate the transmission and control measures [7,22–27].

A nine-dimensional Fasciola mathematical model was studied by M. Diaby et al. [7]. Their results showed that quarantining or treatment alone has little to do with controlling this disease, whereas these two measures could control the further spread of the disease. Turner et al. [23] discussed the partial protection of vaccinations against Fasciola hepatica; this study mainly included their impact on the life cycle and transmission dynamics of the parasite. In his work, Oluwatayo [28] applied the optimal control analysis to preventive measures, hygiene practices, and environmental sanitation that are time-dependent. It was noticed that the combined implementation of these strategies was far more effective in reducing the prevalence of diseases in domestic animals, hence emphasizing the need to apply the above-stated strategies inclusively.

Previous studies focused on the dynamics of the disease. This current research is designed to analyse a deterministic mathematical model with an optimal control framework, considering strategies such as pasture management, treatment of infected cattle, and molluscicide use to derive new insights into the transmission and control of the Fasciola hepatica epidemic. This study will investigate the cost-effectiveness and efficacy of intervention strategies in the spread of Fasciola hepatica.

2. Model formulation and description

We develop a model describing the transmission dynamics of Fasciola hepatica. It considers various life stages of the parasite, the free-living larval stage and intermediate snail host, together with epidemiological conditions in cattle. It provides an overview of the different phases in the life cycle of the disease. First, we consider the cattle population to consist of three subpopulations: susceptible, infected, and treated, denoted by $S_C(t)$, $I_C(t)$, and $T_C(t)$, respectively. Also, there are two classes of snail populations: susceptible snails, denoted by $S_S(t)$, and infected snails, denoted by $I_S(t)$. Lastly, the fasciola larvae population is categorized as miracidium and metacercariae, $M(t)$ and $P(t)$, respectively. The model derives from the following assumptions:

(1) There is no direct disease transmission between the cattle and snail populations.
(2) Climate change does not impact the transmission of the disease.
(3) Treatment leads to recovery but does not provide immunity against reinfection.
(4) The population dynamics of hosts are unaffected by the number of miracidia or metacercariae entering them.
(5) Metacercariae are uniformly distributed across the entire pasture.
(6) Treated cattle are considered non-infectious, meaning they do not contribute to the production of miracidia eggs.

The movement of the cattle population between different classes occurs as their health status changes and the disease progresses. Susceptible cattle are infected when they ingest metacercariae, which can be either encysted on vegetation or freely present in water. Further, susceptible cattle have the potential to contract the disease but have not yet been infected. Infected cattle are those that have consumed metacercariae. Treated cattle encompass those that have undergone treatment for the disease. Here are some additional details of the transition of the disease:

1. Susceptible to infected transition: Susceptible cattle progress to the infected state at a rate of γ_c. This transition occurs when the susceptible cattle consume metacercariae, which is the infectious stage of the parasite found on the pasture.
2. Treatment and recovery: Infected cattle undergo treatment at a rate of δ_c. The treatment aims to combat the infection. Treated cattle then recover from the disease at a rate of λ, indicating their transition back to a susceptible state.
3. Recruitment rates: New cattle and snails are added to the populations through birth rates, Λ_c and Λ_c, respectively.
4. Natural death rate: All cattle compartments: susceptible, infected, and treated cattle experience a natural death rate denoted by μ_c. This accounts for the regular mortality within the cattle population.

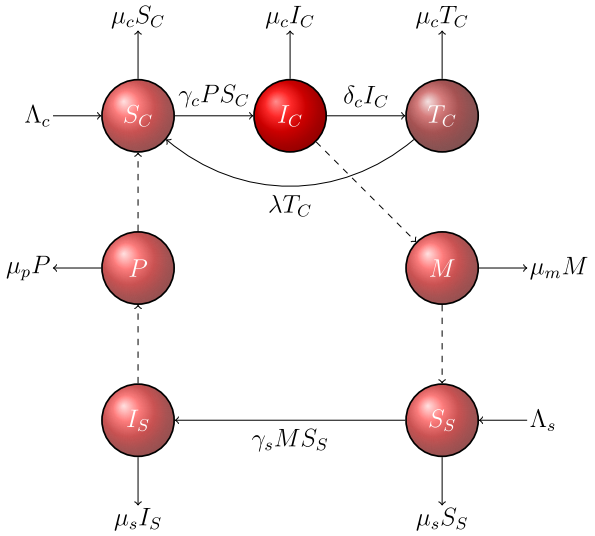

Fig. 1. Transfer diagram for Fasciola hepatica disease.

Table 1
The values and explanations of the parameters used in the model (1).

Parameter	Epidemiological Description	Value	Source
Λ_c	Rate of cattle recruitment	67/day	[7]
Λ_s	Rate of snail recruitment	3000/day	[29]
γ_m	Rate of cattle produce miracidia	6.96 / cattle/day	[29]
γ_p	Rate of snail produce metacercariae	2.6 / snail/day	[29]
γ_c	Per capita infection rate of cattle	0.000000015 /metacer /day	Assumed
γ_s	Per capita infection rate of snails	0.000000012 /miracidia/day	Assumed
δ_c	The rate at which infected cattle are being treated	0.65/day	Assumed
λ	The effectiveness of the treatment in improving the health of infected cattle	0.9567/day	[7]
μ_c	The natural mortality rate of cattle	0.0185/day	[7]
μ_s	The natural mortality rate of snails.	0.001644/day	[7]
μ_m	Natural death rate for miracidia larvae	0.9/day	[29,30]
μ_p	Natural death rate for metacercariae larvae	0.6452/day	[7]

5. Miracidia release and snail penetration: The infected cattle release eggs, which develop into miracidia, a larval form of the parasite. The release of miracidia occurs at a rate of γ_m. A portion of the miracidia population penetrates snails at a rate of γ_s, initiating the next stage of the parasite's life cycle.

Fig. 1 illustrates a graphical overview of the disease's spread and its interactions with the cattle population. Table 1 gives a summary of the system parameters.

From Fig. 1 and the description of terms given in Table 1, the dynamics of the model are as given in the system of equations (1):

$$\begin{cases} S_C'(t) = \Lambda_c - \gamma_c S_C(t)P(t) - \mu_c S_C(t) + \lambda T_C(t), \\ I_C'(t) = \gamma_c S_C(t)P(t) - (\delta_c + \mu_c)I_C(t), \\ T_C'(t) = \delta_c I_C(t) - (\lambda + \mu_c)T_C(t), \\ M'(t) = \gamma_m I_C(t) - \mu_m M(t), \\ S_S'(t) = \Lambda_s - \gamma_s S_S(t)M(t) - \mu_s S_S(t), \\ I_S'(t) = \gamma_s S_S(t)M(t) - \mu_s I_S(t), \\ P'(t) = \gamma_p I_S(t) - \mu_p P(t), \end{cases} \tag{1}$$

where initial conditions, $S_C(0) \geq 0$, $I_C(0) \geq 0$, $T_C(0) \geq 0$, $M(0) \geq 0$, $P(0) \geq 0$, $S_S(0) \geq 0$, and $I_S(0) \geq 0$.

3. Model analysis

3.1. Positive invariant region of the model

We aim to ensure the biological relevance and accurate presentation of the model (1) by rigorously verifying that all fundamental state components start with and maintain positive values throughout the simulation.

Lemma 1. *If all the initial values, $S_C(0)$, $I_C(0)$, $T_C(0)$, $S_S(0)$, $I_S(0)$, $P(0)$, and $M(0)$, are positive, then the solutions to the model (1) will remain non-negative for any positive value of t.*

Proof. We establish this by using the method of reduction to absurdity, considering the set $\{S_C(t), I_C(t), T_C(t), M(t), S_S(t), I_S(t), P(t)\}$ and defining $Q = min\{S_C(t), I_C(t), T_C(t), M(t), S_S(t), I_S(t), P(t)\}$. Contradict the validity of the conclusion presented in Lemma 1. Hence, there is $\tau > 0$ such that $Q(\tau) = 0$, $Q(t) > 0$, for $t \in [0, \tau)$, and $Q(\tau^+) < 0$, for $\tau^+ > \tau$.

If $Q(\tau) = S_C(\tau)$, then all other components of Q become positive. From the first equation of model (1), we obtain

$$\frac{dS_C(\tau)}{dt} = \Lambda_c - \gamma_c S_C(\tau)P(\tau) - \mu_c S_C(\tau) + \lambda T_C(\tau) = \Lambda_c + \lambda T_C(\tau) > 0.$$

Since $\frac{dS_C(\tau)}{dt} > 0$, by applying the property of monotonic functions, it can be concluded that $S_C(\tau^+) > 0$ for $\tau^+ > \tau$. The obtained result contradicts the fact that $S_C(\tau^+) < 0$ for $\tau^+ > \tau$.

Therefore, $S_C(t)$ remains positive for any positive value of t. Furthermore, for any positive value of t, the other state variables also consistently maintain positive values.

Lemma 2. *All possible solutions to model (1) remain within a uniformly bounded region:*

$$\Omega = \left\{ (S_C, I_C, T_C, M, S_S, I_S, P) \in \mathbb{R}^7 : N_C \le \frac{\Lambda_c}{\mu_c}, N_S \le \frac{\Lambda_s}{\mu_s}, M \le \frac{\gamma_m \Lambda_c}{\mu_c \mu_m}, P \le \frac{\gamma_p \Lambda_s}{\mu_s \mu_p} \right\}, \tag{2}$$

where, $N_C(t) = S_C(t) + I_C(t) + T_C(t)$, and $N_S(t) = S_S(t) + I_S(t)$ are the total cattle and snail population at time t.

Proof. Consider the total cattle population in the model (1),

$$\frac{dN_C}{dt} = \Lambda_c - \mu_c N_C. \tag{3}$$

Solving the differential equation (3) leads to the solution

$$N_C(t) = \frac{\Lambda_c}{\mu_c} - \left(\frac{\Lambda_c - \mu_c N_C(0)}{\mu_c} \right) e^{-\mu_c t}.$$

As $t \to \infty$, $N_C(t)$ converges to $\frac{\Lambda_c}{\mu_c}$. If $0 \le N_C(0) \le \frac{\Lambda_c}{\mu_c}$, then

$$0 \le N_C(t) \le \frac{\Lambda_c}{\mu_c}.$$

Applying a similar approach to the snail population results in,

$$0 \le N_S(t) \le \frac{\Lambda_s}{\mu_s}.$$

Furthermore, using this approach and the inequalities $0 \le N_C(t) \le \frac{\Lambda_c}{\mu_c}$ and $0 \le N_S(t) \le \frac{\Lambda_s}{\mu_s}$ for the miracidia and metacercaria populations, we obtain

$$0 \le M(t) \le \frac{\gamma_m \Lambda_c}{\mu_c \mu_m},$$

$$0 \le P(t) \le \frac{\gamma_p \Lambda_s}{\mu_s \mu_p}.$$

This completes the proof, confirming that Ω in (2) defines the feasible region of the system. Therefore, the model is suitable for an epidemiological study [31].

3.2. Disease-free equilibrium (DFE)

The disease-free equilibrium of Fasciola hepatica is a state without infection. This state is denoted as E_0, and is given by

$$E_0 = \left(S_C^0, I_C^0, T_C^0, M^0, S_S^0, I_S^0, P^0\right) = \left(\frac{\Lambda_c}{\mu_c}, 0, 0, 0, \frac{\Lambda_s}{\mu_s}, 0, 0 \right).$$

3.3. Fasciola hepatica reproduction number

The next-generation matrix method, as described by [32], determines the reproduction number in a compartmental model by constructing and analysing a matrix of transitions and interactions between compartments. This method was used and described by the authors in the study [31,33]. In model (1), the compartments I_C, T_C, M, I_S, and P represent various stages or categories of individuals within the infected population. Therefore, the system of differential equations governing these disease compartments can be described as follows:

$$\begin{cases} I_C'(t) &= \gamma_c S_C(t) P(t) - (\delta_c + \mu_c) I_C(t), \\ T_C'(t) &= \delta_c I_C(t) - (\lambda + \mu_c) T_C(t), \\ M'(t) &= \gamma_m I_C(t) - \mu_m M(t), \\ I_S'(t) &= \gamma_s S_S(t) M(t) - \mu_s I_S(t), \\ P'(t) &= \gamma_p I_S(t) - \mu_p P(t). \end{cases} \tag{4}$$

We can express equation (4) as:

$$\frac{d\mathcal{Y}}{dy} = g(\mathcal{Y}) - f(\mathcal{Y}),$$

where $g(\mathcal{Y})$ represents the incidence rate of new incidents appearing in the disease compartments and $f(\mathcal{Y})$ represents the rate at which individuals are moved into and out of the compartments. The variable $\mathcal{Y}$ represents the disease subclass of the system, $\mathcal{Y} = (I_C, T_C, M, I_S, P)$,

$$g = \begin{pmatrix} \gamma_c S_C P \\ 0 \\ 0 \\ \gamma_s S_s M \\ 0 \end{pmatrix}, \text{ and } f = \begin{pmatrix} (\delta_c + \mu_c) I_C \\ -\delta_c I_C + (\lambda + \mu_c) T_C \\ -\gamma_m I_C + \mu_m M \\ \mu_s I_S \\ -\gamma_p I_S + \mu_p P \end{pmatrix}.$$

Computing the derivatives of g and f to the disease variables and evaluating them at the disease-free equilibrium yield the Jacobian matrices G and F.

$$G = \begin{pmatrix} 0 & 0 & 0 & 0 & \frac{\gamma_c \Lambda_c}{\mu_c} \\ 0 & 0 & 0 & 0 & 0 \\ 0 & 0 & 0 & 0 & 0 \\ 0 & 0 & \frac{\gamma_s \Lambda_s}{\mu_s} & 0 & 0 \\ 0 & 0 & 0 & 0 & 0 \end{pmatrix}, \text{ and } F = \begin{pmatrix} \delta_c + \mu_c & 0 & 0 & 0 & 0 \\ -\delta_c & \lambda + \mu_c & 0 & 0 & 0 \\ -\gamma_m & 0 & \mu_m & 0 & 0 \\ 0 & 0 & 0 & \mu_s & 0 \\ 0 & 0 & 0 & -\gamma_p & \mu_p \end{pmatrix}.$$

We define R_0 as the maximum eigenvalue of GF^{-1}. Thus, the threshold quantity is given by $R_0 = \rho(GF^{-1})$. The Fasciola hepatica reproduction number is given as:

$$R_0 = \sqrt{\frac{\gamma_c \gamma_m \gamma_s \gamma_p \Lambda_c \Lambda_s}{\mu_c (\delta_c + \mu_c) \mu_m \mu_p \mu_s^2}}.$$

3.4. Global stability of disease-free equilibrium

Lemma 3. *Castillo-Chávez et al. [34] introduced a novel approach to ascertain the global steady state of the Disease-Free Equilibrium within the positive real domain, $\Omega \in R_+^7$. The model (1) in this context is represented as follows:*

$$\begin{cases} \frac{dX}{dt} &= R(X, Y), \\ \frac{dY}{dt} &= Q(X, Y), Q(X, 0) = 0. \end{cases} \tag{5}$$

Here, $X = (S_C, S_S)$ represents the disease-free subgroups, and $Y = (I_C, T_C, M, I_S, P)$ represents the infectious subgroups. If the following requirements (C_1) and (C_2) are met, then the global stability of E_0 is guaranteed when $R_0 < 1$.

C_1 : *For $\frac{dX}{dt} = R(X, 0)$, the equilibrium point X^* is guaranteed to be stable on a global scale.*
C_2 : $Q(X, Y) = BY - \hat{Q}(X, Y), \hat{Q}(X, Y) \geq 0$ *for $(X, Y) \in \Omega$,*

with $B = D_Y Q(X^*, 0)$ is an M-matrix where the off-diagonal entries of B are nonnegative. The domain Ω represents the set of values for (X, Y) where the model is feasible.

Theorem 1. *The disease-free equilibrium is globally asymptotically stable if $R_0 < 1$ and unstable otherwise.*

Proof. We prove this by applying Lemma 3. Beginning with equation (5), we can derive the following:

$$R(X,0)=\begin{pmatrix}\Lambda_c-\mu_c S_C\\ \Lambda_s-\mu_s S_S\end{pmatrix}. \tag{6}$$

From the disease class system of differential equation (4), we have:

$$Q(X,Y)=BX-\hat{Q}(X,Y),$$

where,

$$B=\begin{pmatrix}-(\delta_c+\mu_c) & 0 & 0 & 0 & \frac{\gamma_c\Lambda_c}{\mu_c}\\ \delta_c & -(\lambda+\mu_c) & 0 & 0 & 0\\ \gamma_m & 0 & -\mu_m & 0 & 0\\ 0 & 0 & \frac{\gamma_s\Lambda_s}{\mu_s} & -\mu_s & 0\\ 0 & 0 & 0 & \gamma_s & -\mu_p\end{pmatrix}.$$

$$\hat{Q}(X,Y)=\begin{pmatrix}P\gamma_c(\frac{\Lambda_c}{\mu_c}-S_C)\\ 0\\ 0\\ M\gamma_s(\frac{\Lambda_s}{\mu_s}-S_S)\\ 0\end{pmatrix}. \tag{7}$$

The global asymptote of equation (6) is $X^*=(\frac{\Lambda_c}{\mu_c},\frac{\Lambda_s}{\mu_s})$ thereby satisfying the condition C_1. Additionally, according to equation (7), $\hat{Q}(X,Y)\geq 0$ for $S_C\leq\frac{\Lambda_c}{\mu_c}$ and $S_S\leq\frac{\Lambda_s}{\mu_s}$. Consequently, $\hat{Q}(X,Y)\geq 0$, for all (X,Y) within the set Ω, confirming condition C_2. The non-diagonal entries of B are non-negative, establishing B as an M-matrix. This proves that the DFE is globally stable whenever $R_0<1$.

3.5. Existence and global stability of endemic equilibrium

The endemic equilibrium point of the model (1) is

$$E_e^*=(S_C^*,I_C^*,T_C^*,M^*,S_S^*,I_S^*,P^*),$$

where

$$S_C^*=\frac{(\delta_c+\mu_c)\mu_p\mu_s(\gamma_m\gamma_s\Lambda_c(\lambda+\mu_c)+\mu_c(\lambda+\delta_c+\mu_c)\mu_m\mu_s)}{\gamma_m\gamma_s\mu_c(\gamma_c\gamma_p\Lambda_s(\lambda+\delta_c+\mu_c)+(\lambda+\mu_c)(\delta_c+\mu_c)\mu_p\mu_s)},$$

$$I_C^*=\frac{A(\lambda+\mu_c)(R_0^2-1)}{\gamma_m\gamma_s\mu_c(\gamma_c\gamma_p\Lambda_s(\lambda+\delta_c+\mu_c)+(\lambda+\mu_c)(\delta_c+\mu_c)\mu_p\mu_s)},$$

$$T_C^*=\frac{\delta_c A(R_0^2-1)}{\gamma_m\gamma_s\mu_c(\gamma_c\gamma_p\Lambda_s(\lambda+\delta_c+\mu_c)+(\lambda+\mu_c)(\delta_c+\mu_c)\mu_p\mu_s)},$$

$$M^*=\frac{A(\lambda+\mu_c)(R_0^2-1)}{\gamma_s\mu_c\mu_m(\gamma_c\gamma_p\Lambda_s(\lambda+\delta_c+\mu_c)+(\lambda+\mu_c)(\delta_c+\mu_c)\mu_p\mu_s)},$$

$$S_S^*=\frac{\mu_c\mu_m(\gamma_c\gamma_p\Lambda_s(\lambda+\delta_c+\mu_c)+(\lambda+\mu_c)(\delta_c+\mu_c)\mu_p\mu_s)}{\gamma_c\gamma_p(\gamma_m\gamma_s\Lambda_c(\lambda+\mu_c)+\mu_c(\lambda+\delta_c+\mu_c)\mu_m\mu_s)},$$

$$I_S^*=\frac{A(\lambda+\mu_c)(R_0^2-1)}{\gamma_c\gamma_p\mu_s(\gamma_m\gamma_s\Lambda_c(\lambda+\mu_c)+\mu_c(\lambda+\delta_c+\mu_c)\mu_m\mu_s)},$$

$$P^*=\frac{A(\lambda+\mu_c)(R_0^2-1)}{\gamma_c\mu_p\mu_s(\gamma_m\gamma_s\Lambda_c(\lambda+\mu_c)+\mu_c(\lambda+\delta_c+\mu_c)\mu_m\mu_s)},$$

such that $A=\mu_c(\delta_c+\mu_c)\mu_m\mu_p\mu_s^2$. This proves that the disease becomes endemic if $R_0>1$.

To determine the global stability of E_e^*, we will check if matrix Q from Equation (9) meets the Volterra-Lyapunov stability conditions. We review the necessary criteria, definitions, and theorems and then construct the Lyapunov function.

Lemma 4. *Suppose Q is a square matrix with n rows and columns, where all the entries are real numbers. If every eigenvalue of Q has a negative (positive) real part, then there exists a positive definite matrix H such that the matrix $HQ+Q^TH^T$ is negative (positive) definite.*

Definition 3.1. An $n \times n$ matrix Q is considered to be Volterra-Lyapunov if there is a positive diagonal matrix M of the same size, such that the expression $MQ+Q^TM^T$ results in a negative definite matrix.

Definition 3.2. If there exists a diagonal matrix M containing only positive values such that the expression $MQ+Q^TM^T$ results in a positive definite matrix, then a square matrix Q is considered to be diagonally stable or positive stable.

Lemma 5. *[35–37] For a non-singular matrix $D = [d_{ij}]$ with dimensions $n \times n$ where $n \geq 2$ and a positive diagonal matrix $M = diag(m_1, m_2, ..., m_n)$ with dimensions $n \times n$, let $E = D^{-1}$. If $d_{nn} > 0$, $\bar{M}\bar{E} + (\bar{M}\bar{E})^T > 0$ and $\bar{M}\bar{D} + (\bar{M}\bar{D})^T > 0$, it is possible to select a value of $m_n > 0$ such that $MD + D^TM^T > 0$.*

It should be noted that to obtain the matrix denoted by $\tilde{A}$ from an n x n matrix A, one should eliminate its final row and final column, which produces a matrix whose size is $(n-1) \times (n-1)$.

Lemma 6. *If matrix A is diagonally stable, then its transpose matrix, A^T, and inverse matrix, A^{-1}, will also be diagonally stable [38].*

Consider the following Lyapunov function:

$$L = \frac{1}{2}[k_1(S_C - S_C^*)^2 + k_2(I_C - I_C^*)^2 + k_3(T_C - T_C^*)^2 + k_3(M - M^*)^2 + k_4(S_S - S_S^*)^2 + k_6(I_S - I_S^*)^2 + k_7(P - P^*)^2],$$

where k_i's are constants with positive values.

$$\frac{dL}{dt} = k_1(S_C - S_C^*)\frac{dS_C}{dt} + k_3(I_C - I_C^*)\frac{dI_C}{dt} + k_4(T_C - T_C^*)\frac{dT_C}{dt} + k_5(M - M^*)\frac{dM}{dt} + k_6(S_S - S_S^*))\frac{dS_S}{dt} + k_8(I_S - I_S^*))\frac{dI_S}{dt} + k_9(P - P^*))\frac{dP}{dt}. \tag{8}$$

Simplifying Equation (8) gives,

$$\frac{dL}{dt} = Y(WQ + Q^TW^T)Y^T,$$

where, $Y = (S_C - S_C^*, I_C - I_C^*, T_C - T_T^*, M - M^*, S_S - S_S^*, I_S - I_S^*, P - P^*)$, $W = diag(w_1, w_2, ..., w_n)$, and

$$Q = \begin{pmatrix} -P^*\gamma_c - \mu_s & 0 & \gamma & 0 & 0 & 0 & -S_C\gamma_c \\ P^*\gamma_c & -\delta_c - \mu_c & 0 & 0 & 0 & 0 & S_C\gamma_c \\ 0 & \delta_c & -\lambda - \mu_c & 0 & 0 & 0 & 0 \\ 0 & \gamma_m & 0 & -\mu_m & 0 & 0 & 0 \\ 0 & 0 & 0 & -S_S\gamma_s & -\mu_s - M^*\gamma_s & 0 & 0 \\ 0 & 0 & 0 & S_S\gamma_s & M^*\gamma_s & -\mu_s & 0 \\ 0 & 0 & 0 & 0 & 0 & \gamma_p & -\mu_p \end{pmatrix}. \tag{9}$$

Theorem 2. *The matrix Q stated in Equation (9) is Volterra–Lyapunov stable.*

Proof. An entry in the last row and column is a positive value. We get the matrix from a $n \times n$ matrix Q, first deleting its last row and column. We need to prove that Lemma 6 holds by showing the diagonal stability of both the matrix $D = -\tilde{Q}$ in Equation (9) and its inverse D^{-1}.

$$D = \begin{pmatrix} P^*\gamma_c + \mu_s & 0 & \gamma & 0 & 0 & 0 \\ -P^*\gamma_c & \delta_c + \mu_c & 0 & 0 & 0 & 0 \\ 0 & -\delta_c & \lambda + \mu_c & 0 & 0 & 0 \\ 0 & -\gamma_m & 0 & \mu_m & 0 & 0 \\ 0 & 0 & 0 & S_S\gamma_s & \mu_s + M^*\gamma_s & 0 \\ 0 & 0 & 0 & -S_S\gamma_s & -M^*\gamma_s & \mu_s \end{pmatrix}. \tag{10}$$

Based on Lemma 5, we assert and provide evidence that both $D = -\tilde{Q}$ and D^{-1} exhibit diagonal stability. This confirms the Volterra-Lyapunov stability of the matrix Q.

Theorem 3. *The matrix D described in equation (10) is diagonally stable.*

Proof. Based on Lemma 5, if we take any sub-matrices, $\tilde{D}_{6\times6}$-$\tilde{D}_{3\times3}$, from a matrix Q by excluding the last row and columns, they will contain a positive diagonal element, $\tilde{d}_{nn} > 0$ (where $3 \leq n \leq 6$). These sub-matrices exhibit diagonal stability, which can be confirmed deductively. Furthermore, their inverses also possess diagonal stability according to Lemma 6. As a result, the matrix $\tilde{D}$ mentioned

Table 2
Normalized forward sensitivity indices.

Parameters	$\Gamma_{\theta}^{R_0}$	Sensitivity indices
Λ_c	$\frac{1}{2}$	+0.5
Λ_s	$\frac{1}{2}$	+0.5
μ_c	$-(\delta_c + 2\mu_c)/(2(\delta_c + \mu_c))$	-0.5023
μ_s	-1	-1
μ_m	$-\frac{1}{2}$	-0.5
μ_p	$-\frac{1}{2}$	-0.5
γ_m	$\frac{1}{2}$	+0.5
γ_p	$\frac{1}{2}$	+0.5
γ_c	$\frac{1}{2}$	+0.5
γ_s	$\frac{1}{2}$	+0.5
δ_c	$-\delta_c/2(\delta_c + \mu_c)$	-0.4977

in Equation (10) is guaranteed to be diagonal stable. The fact that the matrix $\tilde{D} = -\tilde{Q}$ is diagonally stable means that, according to Definition 3.2, there is a positive diagonal matrix M such that $M\tilde{D} + \tilde{D}^T M^T > 0$. Additionally, replacing $\tilde{D}$ with $-\tilde{Q}$ shows that $M\tilde{Q} + \tilde{Q}^T M^T$ is less than zero, indicating that Q is Volterra-Lyapunov stable based on Definition 3.1.

As a result of the following three conditions satisfied:
(i) $a_{11} = -P^*\gamma_c - \mu_s < 0$, (ii) $a_{22} = -\delta_c - \mu_c < 0$, and (iii) $det(Q_{2\times2}) = (P^*\gamma_c - \mu_s)(-\delta_c - \mu_c) > 0$, the matrix

$$\tilde{Q}_{2\times2} = \begin{pmatrix} -P^*\gamma_c - \mu_s & 0 \\ -P^*\gamma_c & -\delta_c - \mu_c \end{pmatrix},$$

which is found from a matrix Q is Voltera Lyapunov stable.

The matrix $\tilde{D}_{2\times2}$, which is equal to the negation of $\tilde{Q}_{2\times2}$, demonstrates diagonal stability. This implies that both the matrix D from Equation (10) and its inverse matrix also possess diagonal stability. Therefore, the matrix Q mentioned in Equation (9) can be considered Volterra-Lyapunov stable. In summary, the following theorem can be derived from the previous discussions.

Theorem 4. *The endemic equilibrium E_e^* of Model (1) is globally asymptotically stable for $R_0 > 1$.*

Proof. According to Theorem 2, a positive diagonal matrix Y exists such that the expression $YA + A^T Y^T$ is negative. Therefore, if X, in Equation (8), is not equal to the endemic equilibrium point E_e^*, then the derivative of the Lyapunov function $\frac{dL}{dt}$ will be negative. This ensures the global stability of the endemic equilibrium point.

4. Sensitivity analysis

Sensitivity analysis is a crucial tool in epidemiology that allows researchers to understand the relative importance of different parameters in a model and their impact on critical outcomes [39]. One commonly used metric for this analysis is the normalized sensitivity index, denoted as $\Gamma_{\theta}^{R_0}$, which quantifies the percentage change of R_0 to the parameter θ [40]. It is given by

$$\Gamma_{\theta}^{R_0} = \frac{\partial R_0}{\partial \theta} \cdot \frac{\theta}{R_0}.$$

The sensitivity analysis results, as presented in Table 2 and illustrated in Fig. 2, provide valuable insights into the parameters influencing the basic reproduction number (R_0) of fasciola hepatica infection in cattle. The analysis identifies several key findings. Firstly, recruitment rates, miracidia, and metacercariae production rates, and transmission rates between cattle and snails are the most sensitive parameters directly impacting R_0. These parameters play a significant role in shaping the severity and transmission dynamics of the infection in cattle. Additionally, the sensitivity analysis highlights the indirect effects of mortality rates in miracidia, metacercariae, and snail populations and the treatment rate of infected cattle on R_0. Among these factors, the snail mortality rate emerges as the most influential parameter with an indirect effect on R_0. To effectively control the spread of fasciola hepatica in cattle, stakeholders should focus on increasing treatment rates and implementing measures to control mortality rates within the snail, miracidia, and metacercariae populations. By targeting these influential parameters, it is possible to mitigate the burden of the infection and prevent its further transmission among cattle.

5. Optimal control analysis

Optimal control theory is an area of mathematics that seeks optimal techniques to govern a dynamic system over time to optimize an objective function [41]. After analysing the sensitivity results, we concentrate on the control variable $u_1(t)$, which represents pasture management aimed at reducing the risk of cattle infection from metacercariae. Similarly, $u_2(t)$ pertains to measures for treating cattle, and $u_3(t)$ quantifies efforts to control snails using molluscicide to mitigate Fasciola hepatica disease. By integrating these control variables into the model, we derive the following formulation:

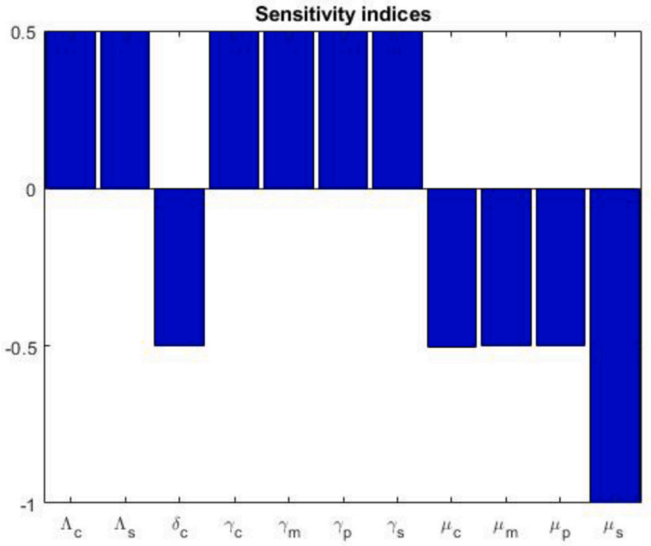

Fig. 2. Parameter sensitivity analysis.

$$\begin{cases} S_C'(t) = \Lambda_c - (1-u_1(t))\gamma_c S_C(t)P(t) - \mu_c S_C(t) + \lambda T_C(t), \\ I_C'(t) = (1-u_1(t))\gamma_c S_C(t)P(t) - (\delta_c + u_2(t) + \mu_c)I_C(t), \\ T_C'(t) = (\delta_c + u_2(t))I_C(t) - (\lambda + \mu_c)T_C(t), \\ M'(t) = \gamma_m I_C(t) - \mu_m M(t), \\ S_S'(t) = \Lambda_s - \gamma_s S_S(t)M(t) - (\mu_s + u_3(t))S_S(t), \\ I_S'(t) = \gamma_s S_S(t)M(t) - (\mu_s + u_3(t))I_S(t), \\ P'(t) = \gamma_p I_S(t) - \mu_p P(t), \end{cases} \tag{11}$$

subject to initial conditions of the model (1).

Nonlinear control interventions are used because of the nonlinear costs of healthcare prevention measures [28,42]. We aim to decrease the number of infected cattle, manage the snail population, and minimize the costs of these interventions. The objective function, representing the cost of these interventions, is defined as follows:

$$J(u_1,u_2,u_3) = \int_0^{t_f} (A_1 I_C + A_2 N_S + \frac{1}{2}C_1 u_1^2 + \frac{1}{2}C_2 u_2^2 + \frac{1}{2}C_3 u_3^2)\, dt, \tag{12}$$

where A_1 and A_2 are positive weights used to balance the factors related to the number of infected cattle, and the total snail population, respectively. Likewise, C_1, C_2, and C_3 denote the weights assigned to the costs of the control programs throughout t_f days, which represents the time frame for implementing the control strategy.

The objective is to identify the optimal controls, u_1^*, u_2^*, and u_3^* that satisfy the following condition:

$$J(u_1^*,u_2^*,u_3^*) = \lim_{\mathcal{U}} J(u_1,u_2,u_3), \tag{13}$$

where the control set $\mathcal{U}$ is Lebesgue measurable, and it is defined as follows:

$$\mathcal{U} = \{u : 0 \le u_1(t) \le 1, 0 \le u_2(t) \le 1, 0 \le u_3(t) \le 1, \text{for} \quad t \in [0,t_f]\}.$$

5.1. Existence of an optimal control

Theorem 5. *For Equation (13) to be valid, it is required to fulfil the following conditions A–D. These conditions are necessary to identify an optimal control (u_1^*,u_2^*,u_3^*) that minimizes the objective functional $J(u_1,u_2,u_3)$ while satisfying the constraints of the control model (11).*

(A) *The admissible control set $\mathcal{U}$ must be both convex and closed.*
(B) *The control system must be bounded by a linear function involving the state and control variables.*
(C) *The integrand of the objective functional in (12) must exhibit convexity with respect to the controls.*

(D) *The Lagrangian must be bounded below by*

$$a_0\left(\sum_{i=1}^{3}|u_i|^2\right)^{\frac{a_2}{2}} - a_1,$$

where $a_0 > 0$, $a_1 > 0$, *and* $a_2 > 1$.

Proof. To establish the existence of an optimal control (u_1^*, u_2^*, u_3^*), we assign the right-hand side of the system (11) as $f(t, \mathcal{X}, u)$, where $\mathcal{X} = (S_C, I_C, T_C, M, S_S, I_S, P)$, $u = (u_1, u_2, u_3) \in \mathcal{U} = [0,1] \times [0,1] \times [0,1]$ and

$$f(t,\mathcal{X},u) = \begin{pmatrix} \Lambda_c - (1-u_1(t))\gamma_c S_C(t)P(t) - \mu_c S_C(t) + \lambda T_C(t) \\ (1-u_1(t))\gamma_c S_C(t)P(t) - (\delta_c + u_2(t) + \mu_c)I_C(t) \\ (\delta_c + u_2(t))I_C(t) - (\lambda + \mu_c)T_C(t) \\ \gamma_m I_C(t) - \mu_m M(t) \\ \Lambda_s - \gamma_s S_S(t)M(t) - (\mu_s + u_3(t))S_S(t) \\ \gamma_s S_S(t)M(t) - (\mu_s + u_3(t))I_S(t) \\ \gamma_p I_S(t) - \mu_p P(t) \end{pmatrix}. \tag{14}$$

Following the approach outlined in [43], we proceed to verify the satisfaction of the essential conditions.

(A) By definition, it is clear that the control set $\mathcal{U}$ exhibits the property of closure.

Let $v = (v_1, v_2, v_3)$, and $w = (w_1, w_2, w_3)$ represent arbitrary elements belonging to $\mathcal{U}$. Consequently, based on the definition of a convex set, it can be inferred that

$$(1-t)v + tw \in \mathcal{U} \quad \text{for all} \quad t \in [0,1].$$

Let's take two arbitrary corresponding coordinates, v_i and w_i, such that $0 \le v_i \le 1$ and $0 \le w_i \le 1$. For any value of t between 0 and 1, the convex combination $(1-t) * v_i + t * w_i$ lies within the interval [0, 1]. As a result, the expression $(1-t)v + tw$ belongs to $\mathcal{U}$, indicating the convexity of $\mathcal{U}$.

(B) It can be demonstrated that there are functions g and h such that

$$f(t,\mathcal{X},u) = g(t,\mathcal{X}) + h(t,\mathcal{X})u, \tag{15}$$

where, $f(t,\mathcal{X},u)$ is in (14), and

$$g(t,\mathcal{X}) = \begin{pmatrix} \Lambda_c - \gamma_c S_C(t)P(t) - \mu_c S_C(t) + \lambda T_C(t) \\ \gamma_c S_C(t)P(t) - (\delta_c + \mu_c)I_C(t) \\ \delta_c I_C(t) - (\lambda + \mu_c)T_C(t) \\ \gamma_m I_C(t) - \mu_m M(t) \\ \Lambda_s - \gamma_s S_S(t)M(t) - \mu_s S_S(t) \\ \gamma_s S_S(t)M(t) - \mu_s I_S(t) \\ \gamma_p I_S(t) - \mu_p P(t) \end{pmatrix},$$

$$h(t,\mathcal{X},u) = \begin{pmatrix} \gamma_c S_C(t)P(t) & 0 & 0 \\ -\gamma_c S_C(t)P(t) & -I_C(t) & 0 \\ 0 & I_C(t) & 0 \\ 0 & 0 & 0 \\ 0 & 0 & -S_S(t) \\ 0 & 0 & -I_S(t) \\ 0 & 0 & 0 \end{pmatrix}.$$

Applying the norm inequality stated in Equation (15) yields that

$$|f(t,\mathcal{X},u)| \le |g(t,\mathcal{X})| + |h(t,\mathcal{X})||u|.$$

The functions g and h are continuous for the state variables, and each state variable is constrained; it becomes evident that both $|g|$ and $|h|$ are bounded functions. This implies that there exist numbers a and b such that $|g| \le a$ and $|g| \le b$.

This provides,

$$\begin{aligned} |f(t,\mathcal{X},u)| &\le |g(t,\mathcal{X})| + |h(t,\mathcal{X})||u| \\ &\le a + b|u| \\ &\le Max\{a,b\}(1+|u|). \end{aligned}$$

Therefore, $||f(t,\mathcal{X},u)|| \le c(1+|u|)$, where $c = max\{a,b\}$. This demonstrates that condition (B) is fulfilled.

(C) Initially, it is important to observe that the objective function (12), possesses an integrand with characteristics similar to that of the Lagrangian form.

$$\mathcal{L} = A_1 I_C + A_2 N_S + \frac{1}{2}C_1 u_1^2 + \frac{1}{2}C_2 u_2^2 + \frac{1}{2}C_3 u_3^2. \tag{16}$$

Assume $v = (v_1, v_2, v_3)$ and $w = (w_1, w_2, w_3)$ be to arbitrary elements of $\mathcal{U}$, $\lambda \in [0,1]$ then it is necessary to prove that

$$\mathcal{L}(t, \mathcal{X}, (1-\lambda)v + \lambda w) \leq (1-\lambda)\mathcal{L}(t, \mathcal{X}, v) + \lambda(\mathcal{L}(t, \mathcal{X}, w).$$

$$\mathcal{L}(t, \mathcal{X}, (1-\lambda)v + \lambda w) = A_1 I_C + A_2 N_S + \frac{1}{2}\sum_{i=1}^{3}\left(C_i((1-\lambda)v_i + \lambda w_i)\right)^2. \tag{17}$$

Also, we have,

$$(1-\lambda)\mathcal{L}(t, \mathcal{X}, v) + \lambda(\mathcal{L}(t, \mathcal{X}, w) = A_1 I_C + A_2 N_S + \frac{1}{2}(1-\lambda)\sum_{i=1}^{3} C_i v_i^2 + \frac{1}{2}\lambda\sum_{i=1}^{3} C_i w_i^2. \tag{18}$$

Subtracting equation (18) from equation (17)

$$\mathcal{L}(t, \mathcal{X}, (1-\lambda)v + \lambda w) - \left((1-\lambda)\mathcal{L}(t, \mathcal{X}, v) + \lambda(\mathcal{L}(t, \mathcal{X}, w)\right) = \frac{1}{2}(\lambda^2 - \lambda)\sum_{i=1}^{3} C_i(v_i - w_i)^2 \leq 0$$

Since λ is in the interval $[0,1]$, the right-hand side of the equation is nonpositive. Therefore, $\mathcal{L}$ is a convex function.

(D) Furthermore, it is evident that there exists a value $a_2 > 1$, along with positive numbers a_1 and a_0, which satisfy the given conditions:

$$\begin{aligned}
\mathcal{L} = A_1 I_C + A_2 N_S + \frac{1}{2}C_1 u_1^2 + \frac{1}{2}C_2 u_2^2 + \frac{1}{2}C_3 u_3^2 &\geq \frac{1}{2}(C_1 u_1^2 + C_2 u_2^2 + C_3 u_3^2) \\
&\geq \frac{1}{2} min\{C_1, C_2, C_3\}\left(u_1^2 + u_2^2 + u_3^2\right) \\
&\geq \frac{1}{2} min\{C_1, C_2, C_3\}\left(u_1^2 + u_2^2 + u_3^2\right) - a_1 \\
&= a_0\left(u_1^2 + u_2^2 + u_3^2\right)^{\frac{a_2}{2}} - a_1,
\end{aligned}$$

where $a_2 = 2$, $a_1 > 0$, and $a_0 = \frac{1}{2}\min\{C_1, C_2, C_3\}$. This implies that

$$\mathcal{L} \geq a_0\left(u_1^2 + u_2^2 + u_3^2\right)^{\frac{a_2}{2}} - a_1.$$

Therefore, the Lagrangian is bounded below by $a_0\left(\sum_{i=1}^{3}|u_i|^2\right)^{\frac{a_2}{2}} - a_1$, where $a_0 > 0$, $a_1 > 0$, and $a_2 > 1$.

5.2. Characterization of the optimal control problem

To solve the above-formulated problem of optimal control, we use Pontryagin's maximum principle, described in studies [44,45]. This principle provides the necessary conditions for optimal control. With this principle, we can convert differential equations (11) and (16) into problems of Hamiltonian minimization concerning control variables (u_1, u_2, u_3), which gives the conditions for optimality of control. This generally involves the search for a control strategy that minimizes a cost function subject to some constraints; this can be rephrased in terms of a Lagrangian function L as defined by (16), which includes both the cost function and the constraints. Using a Hamiltonian function $\mathcal{H}$, the control problem can be expressed as:

$$\mathcal{H} = \mathcal{L} + \delta_1\frac{dS_C}{dt} + \delta_2\frac{dI_C}{dt} + \delta_3\frac{dT_C}{dt} + \delta_4\frac{dM}{dt} + \delta_5\frac{dS_S}{dt} + \delta_6\frac{dI_S}{dt} + \delta_7\frac{dP}{dt}.$$

The notation δ_i for $i = 1$ to 7 indicates seven adjoint variables corresponding to the state equations S_C, I_C, T_c, M, S_S, I_S, and P. Simplifying the Hamiltonian function results in a more concise form.

$$\begin{aligned}
\mathcal{H} = {} & A_1 I_C + A_2 N_S + \frac{1}{2}[C_1 u_1^2 + C_2 u_2^2 + C_3 u_3^2] + \delta_1[\Lambda_c - (1-u_1)\gamma_c S_C P - \mu_c S_C + \lambda T_C] \\
& + \delta_2[(1-u_1)\gamma_c S_C P - (\delta_c + u_2 + \mu_c)I_C] + \delta_3[(\delta_c + u_2)I_C - (\lambda + \mu_c)T_c] \\
& + \delta_4[\gamma_m I_C - \mu_m M] + \delta_5[\Lambda_s - \gamma_s S_S M - (\mu_s + u_3)S_S] \\
& + \delta_6[\gamma_s S_S M - (\mu_s + u_3)I_S] + \delta_7[\gamma_p I_S - \mu_p P].
\end{aligned} \tag{19}$$

Theorem 6. *The optimal control variables, $u_1^*(t)$, $u_2^*(t)$, and $u_3^*(t)$, along with the solutions $\mathcal{X} := (S_C, I_C, T_C, M, S_S, I_S, P)$ of the state system in equation (1), are associated with adjoint variables δ_i (where i ranges from 1 to 7), which satisfy*

$$\frac{d\delta}{dt} = -\frac{\partial \mathcal{H}(t, \mathcal{X}, u, \delta)}{\partial \mathcal{X}},$$

with transversality conditions $\delta_i(t_f) = 0, i = 1, 2, ..., 7$.

Additionally, the optimality conditions for the problem are given by

$$\left.\begin{aligned} u_1^* &= max\{0, min\{1, \frac{(\delta_2 - \delta_1)\gamma_c S_C P}{C_1}\}\} \\ u_2^* &= max\{0, min\{1, \frac{(\delta_2 - \delta_3) I_C}{C_2}\}\} \\ u_3^* &= max\{0, min\{1, \frac{(\delta_5 S_S + \delta_6 I_S)}{C_3}\}\} \end{aligned}\right\}.$$

Proof. If $(\mathcal{X}, u)$ denotes an optimal solution for an optimal control problem, then the existence of a nontrivial vector function $\delta = (\delta_1, \delta_2, \delta_3, \delta_4, \delta_5, \delta_6, \delta_7)$ is guaranteed. This vector function satisfies the following set of equations.

$$\frac{d\delta}{dt} = -\frac{\partial \mathcal{H}(t, \mathcal{X}, u, \delta)}{\partial \mathcal{X}},$$

where $\mathcal{X} = (S_C, I_C, T_C, M, S_S, I_S, P)$, with transversality conditions: $\delta_i(t_f) = 0, i = 1, 2, ..., 7$.
Therefore, the corresponding adjoint system can be expressed as:

$$\begin{cases} \frac{d\delta_1}{dt} = \gamma_c(1 - u_1)P(\delta_1 - \delta_2) + \mu_c\delta_1, \\ \frac{d\delta_2}{dt} = -A_1 + (\delta_c + u_2 + \mu_c)\delta_2 - (\delta_c + u_2)\delta_3 - \gamma_m\delta_4, \\ \frac{d\delta_3}{dt} = -\lambda\delta_1 + (\lambda + \mu_c)\delta_3, \\ \frac{d\delta_4}{dt} = \mu_m\delta_4 + (\gamma_s S_S)(\delta_5 - \delta_6), \\ \frac{d\delta_5}{dt} = -A_2 + \gamma_s M(\delta_5 - \delta_6) + (\mu_s + u_3)\delta_5, \\ \frac{d\delta_6}{dt} = -A_2 + (\mu_s + u_3)\delta_6 - \gamma_p\delta_7, \\ \frac{d\delta_7}{dt} = \gamma_c(1 - u_1)(\delta_1 - \delta_2)S_C + \mu_p\delta_7. \end{cases}$$

To derive the optimality conditions, we calculate the derivative of the Hamiltonian function (19) for the control variables and solve for the point where the derivative is zero.

$$\frac{\partial \mathcal{H}(t, \mathcal{X}, u, \delta)}{\partial u} = 0.$$

This leads to the following expression:

$$\begin{cases} \frac{\partial \mathcal{H}}{\partial u_1} = C_1 u_1 + (\delta_1 - \delta_2)\gamma_c S_C P = 0, \\ \frac{\partial \mathcal{H}}{\partial u_2} = C_2 u_2 + (\delta_3 - \delta_2) I_C = 0, \\ \frac{\partial \mathcal{H}}{\partial u_3} = C_1 u_1 - \delta_5 S_S - \delta_6 I_S = 0. \end{cases}$$

Solving the equations for $u_1^*(t)$, $u_2^*(t)$, and $u_3^*(t)$, we can draw the following conclusion:

$$u_1^* = max\{0, min\{1, \frac{(\delta_2 - \delta_1)\gamma_c S_C P}{C_1}\}\},$$
$$u_2^* = max\{0, min\{1, \frac{(\delta_2 - \delta_3) I_C}{C_2}\}\},$$
$$u_3^* = max\{0, min\{1, \frac{(\delta_5 S_S + \delta_6 I_S)}{C_3}\}\}.$$

6. Numerical simulations and discussions

We will present the results of numerical simulations performed to analyse both the local and global stabilities of the non-control model, as well as simulations addressing the optimal control problem. Additionally, we will compare the outcomes under two different

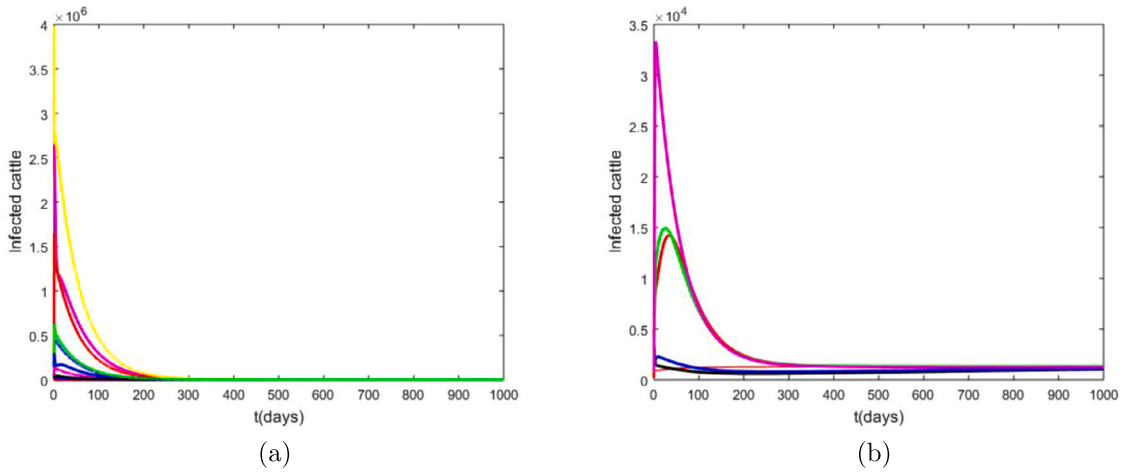

Fig. 3. The global stability of the dynamics of infected cattle in the absence of intervention strategies: (a) Global stability of disease-free equilibrium and (b) Global stability of endemic equilibrium.

scenarios: one incorporating optimal control and the other involving no control at all. The simulations were conducted using the parameter values specified in Table 1.

6.1. Global stability in the absence of intervention strategies

The model was analysed in the absence of intervention strategies to ascertain the progression of the disease dynamics in cattle. Fig. 3 indicates that both the Fascia-free equilibrium and the endemic equilibrium demonstrate global stability. The global stability of the Fasciola hepatica-free equilibrium implies that the parasitic liver fluke cannot establish or maintain an infection in cattle over time. This suggests that the factors affecting the parasite's transmission and survival are not conducive to its spread or persistence. The global stability of the Fasciola hepatica endemic equilibrium indicates that the parasite has established a long-term relationship with its hosts, likely evolving strategies to ensure its survival without causing severe harm.

6.2. Optimal control simulation

The fourth-order Runge-Kutta backward scheme is used to solve the control model numerically. The optimal control simulation is conducted for 100 days. The values for weight constants and cost constants used in the simulations are $A_1 = 800$, $A_2 = 500$, $C_1 = 100$, $C_2 = 85$, and $C_3 = 90$. To see the impact that each control measure has on the eradication of the Fasciola hepatica disease, we assessed the efficiency of four control strategies. Our objective was to determine the most favourable mix of such interventions.

Strategy A: Pasture management (u_1) and cattle treatment (u_2).
Strategy B: Pasture management (u_1) and molluscicides (u_3).
Strategy C: Cattle treatment (u_2) and molluscicides (u_3).
Strategy D: Combine all three controls.

6.2.1. Strategy A: optimal use of pasture management and cattle treatment

In this case, shown in Fig. 4, pasture management (u_1) and treatment of infected cattle (u_2) will optimize the objective function J while setting the value of the molluscicide control (u_3) at zero. Fig. 4(a) indicates that the simultaneous implementation of pasture management and cattle treatment interventions results in an elevated number of susceptible cattle compared to the non-control group. In contrast, Fig. 4(b) illustrates that the implementation of these combined interventions leads to a decrease in the number of cattle infected with the disease. Fig. 4(c) shows that the number of treated cattle initially increases over the first five days but then gradually decreases to zero. Fig. 4(e) indicates that this approach necessitates maintaining maximum cattle treatment throughout almost the entire intervention period, while pasture management should be at its peak during the initial 50 days and then gradually diminish to zero. Studies [46,47] confirm that effective pasture management and regular anthelmintic treatment for infected cattle significantly reduce disease prevalence and transmission.

6.2.2. Strategy B: optimal use of pasture management (u_1) and molluscicides (u_3)

Fig. 5 presents the simulation results of the optimal use of pasture management (u_1) and molluscicides (u_3). Fig. 5(a) highlights a significant contrast in the count of susceptible cattle between the control and non-control models, underscoring the effectiveness of this strategy. The observations from Figs. 5(b), 5(c) and 5(d) further support this, showing a substantial reduction in the total number of infected cattle (I_C), treated cattle (T_C) and the total snail population (N_S) are significantly reduced when the optimal controls are employed, in contrast to in the absence of controls. As shown in Fig. 5(e), this strategy requires maintaining the control profile

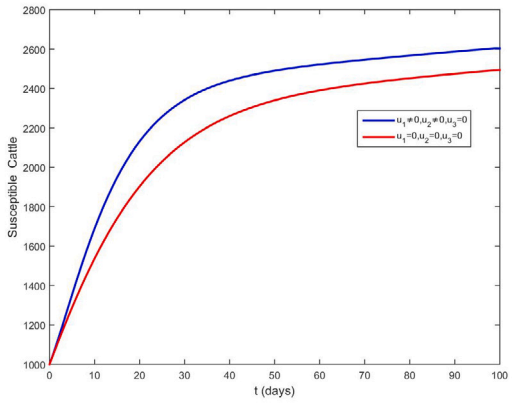

(a)

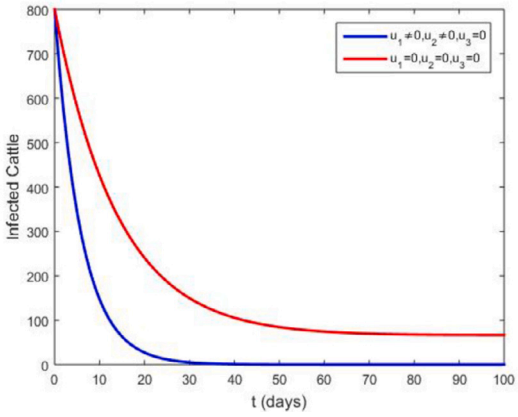

(b)

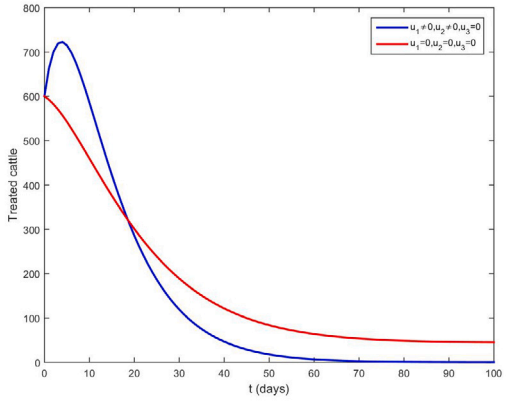

(c)

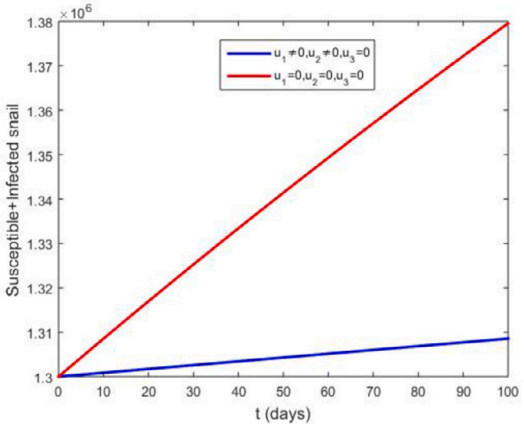

(d)

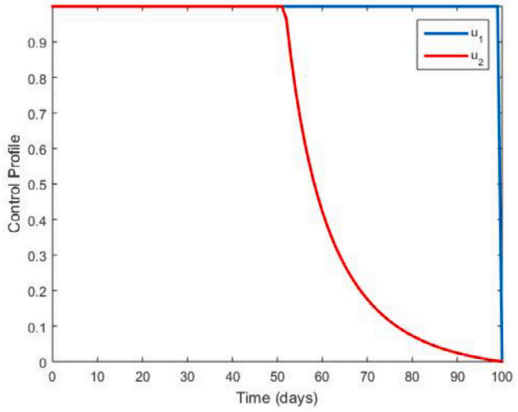

(e)

Fig. 4. The optimal combined effect of implementing pasture management ($u_1(t)$) and cattle treatment ($u_2(t)$) for: (a) susceptible cattle, (b) infected cattle, (c) treated cattle, (d) total snail, and (e) control profile.

for pasture management (u_1) and the use of molluscicides (u_3) at their maximum levels for approximately 90% and 95% of the 100 days, respectively.

6.2.3. Strategy C: optimal use of treatment (u_2) and molluscicides (u_3)

In order to minimize the objective functional J, we perform simulations in Fig. 6 representing the treatment of infected cattle (u_2) combined with molluscicide use while setting the pasture management (u_3) practice to zero. It is noted from Fig. 6(a) that the number of susceptible cattle rises due to controls in comparison with a model with no controls. Furthermore, Fig. 6(b) shows that under control, the number of cattle infected by fasciola hepatica drops dramatically. It is also evident from Fig. 6(c) that the number of treated cattle increases tremendously in the case with controls, especially within a very short time. Fig. 6(d) illustrates a substantial decline in the snail population when implementing this control strategy. Fig. 6(e) additionally illustrates the control profiles for the treatment of infected cattle (u_2) and molluscicides (u_3). The analysis suggests that the treatment control consistently maintains its upper bound of 100% for 95 days. On the other hand, the molluscicide control reaches its maximum level of 100% throughout the entire implementation period.

6.2.4. Strategy D: optimal use of pasture management, treatment, and molluscicides

Under this strategy shown in Fig. 7, we use all three controls, namely u_1, u_2, and u_3, to optimize the objective function J. Fig. 7(a) depicts the use of controls in the model solution results in a more pronounced rise in the number of susceptible cattle compared to the non-control model solution. Including recovered cattle within the susceptible population can account for this phenomenon. Figs. 7(b), 7(c), and 7(d) illustrate that all three of these optimal controls must be used in concert in order to eradicate the disease in both the cattle and snail populations. In Fig. 7(e), in which pasture management is maintained strictly at a maximum level of 100% for 95 days, administering treatment is at a maximum of 100% for 52 days. The possibility of molluscicide control continuously stays at a maximum level of 100% until the end of 100 days, when the optimum solution may be attained. It is highly effective when these three controls are put together to reduce infected cattle, compared to a combination of two control measures.

6.3. Cost-effectiveness analysis

The cost-effectiveness analysis will balance the costs against outcomes to guide resource allocation and policy decision-making for infection control by Fasciola hepatica in cattle. An incremental cost-effectiveness ratio was used in a cost-effectiveness analysis comparing the differences in total costs with a view to indicating the best strategy for controlling Fasciola hepatica in cattle. The ICER may be defined as the ratio of the difference in cost between strategies i and j, divided by the difference in the number of averted infections between those strategies [48,49]. Hence, when two competing strategies are being compared, strategy with i and strategy, say with j, where strategy is more effective than strategy, the computation of ICER values is as follows:

$$ICER = \frac{TC(i)}{TA(i)}.$$

$$ICER(j) = \frac{TC(j) - TC(i)}{TA(j) - TA(i)}.$$

Here the total costs (TC) and the total cases averted (TA), during a given period for strategy i for $i = A, B, C, D$.

Based on the simulation results, we arrange the control strategies in ascending order of effectiveness in terms of infections averted. This ranking procedure reveals that Strategy D resulted in the lowest number of infections averted, followed by Strategies A, C, and B (Table 3). Using this ranking, we initially compare the ICER between Strategy D and Strategy A as follows:

$$ICER(D) = \frac{9.6074 \times 10^5}{5.1348 \times 10^3} = 187.202.$$

$$ICER(A) = \frac{6.2737 \times 10^5 - 9.6074 \times 10^5}{5.1369 \times 10^3 - 5.1348 \times 10^3} = -15879.5238.$$

The lower ICER for strategy A indicates that strategy D is strongly dominated by strategy A. It can be inferred that Strategy A is more cost-effective than Strategy D. As a result, Strategy D is deemed unsuitable, and the analysis proceeds by evaluating the comparison between Strategy A and Strategy C.

$$ICER(A) = \frac{6.2737 \times 10^5}{5.1369 \times 10^3} = 122.087.$$

$$ICER(C) = \frac{6.4329 \times 10^5 - 6.2737 \times 10^5}{5.6423 \times 10^3 - 5.1369 \times 10^3} = 31.521.$$

Based on this inference, it can be concluded that Strategy A is both more expensive and less effective compared to Strategy C. Consequently, Strategy A is eliminated from further analysis, and the focus shifts to comparing Strategy C with Strategy B.

$$ICER(C) = \frac{6.4329 \times 10^5}{5.6423 \times 10^3} = 113.989.$$

$$ICER(B) = \frac{7.1606 \times 10^5 - 6.4329 \times 10^5}{1.2289 \times 10^4 - 5.6423 \times 10^3} = 12.88.$$

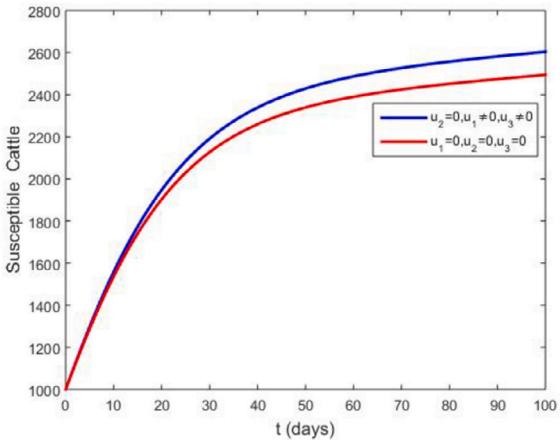

(a)

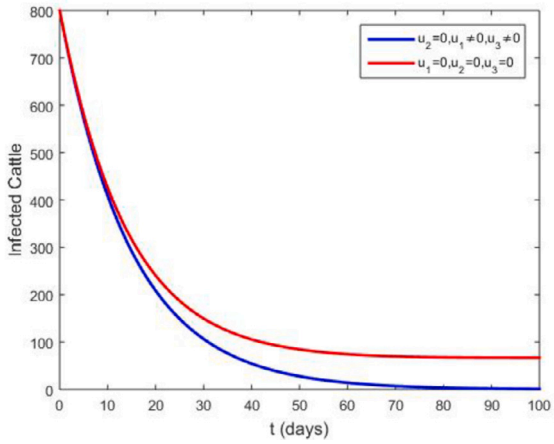

(b)

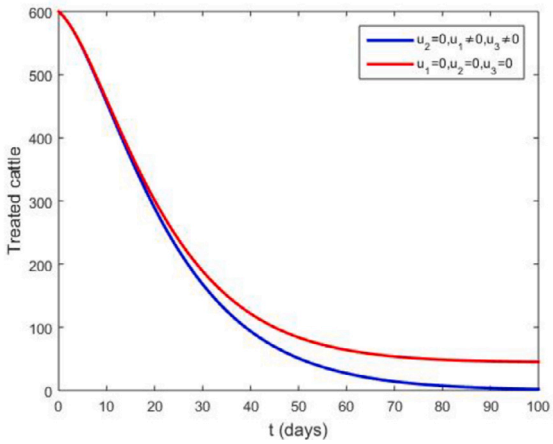

(c)

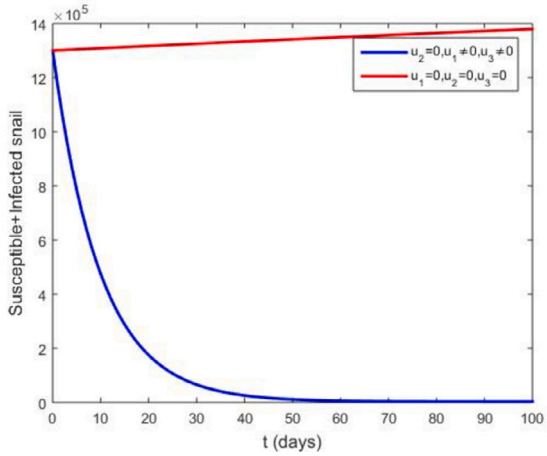

(d)

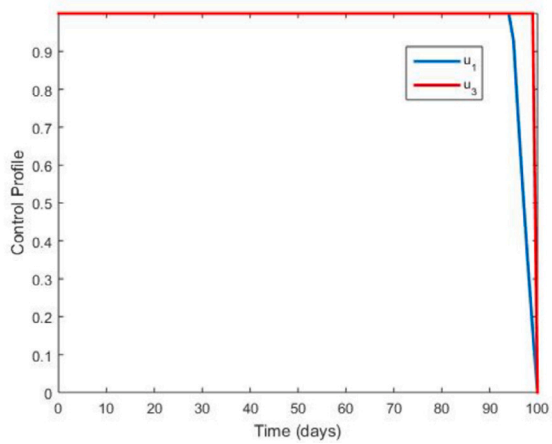

(e)

Fig. 5. The optimal combined effect of implementing pasture management ($u_1(t)$) and molluscicides ($u_3(t)$) for: (a) susceptible cattle, (b) infected cattle, (c) treated cattle, (d) total snail, and (e) control profile.

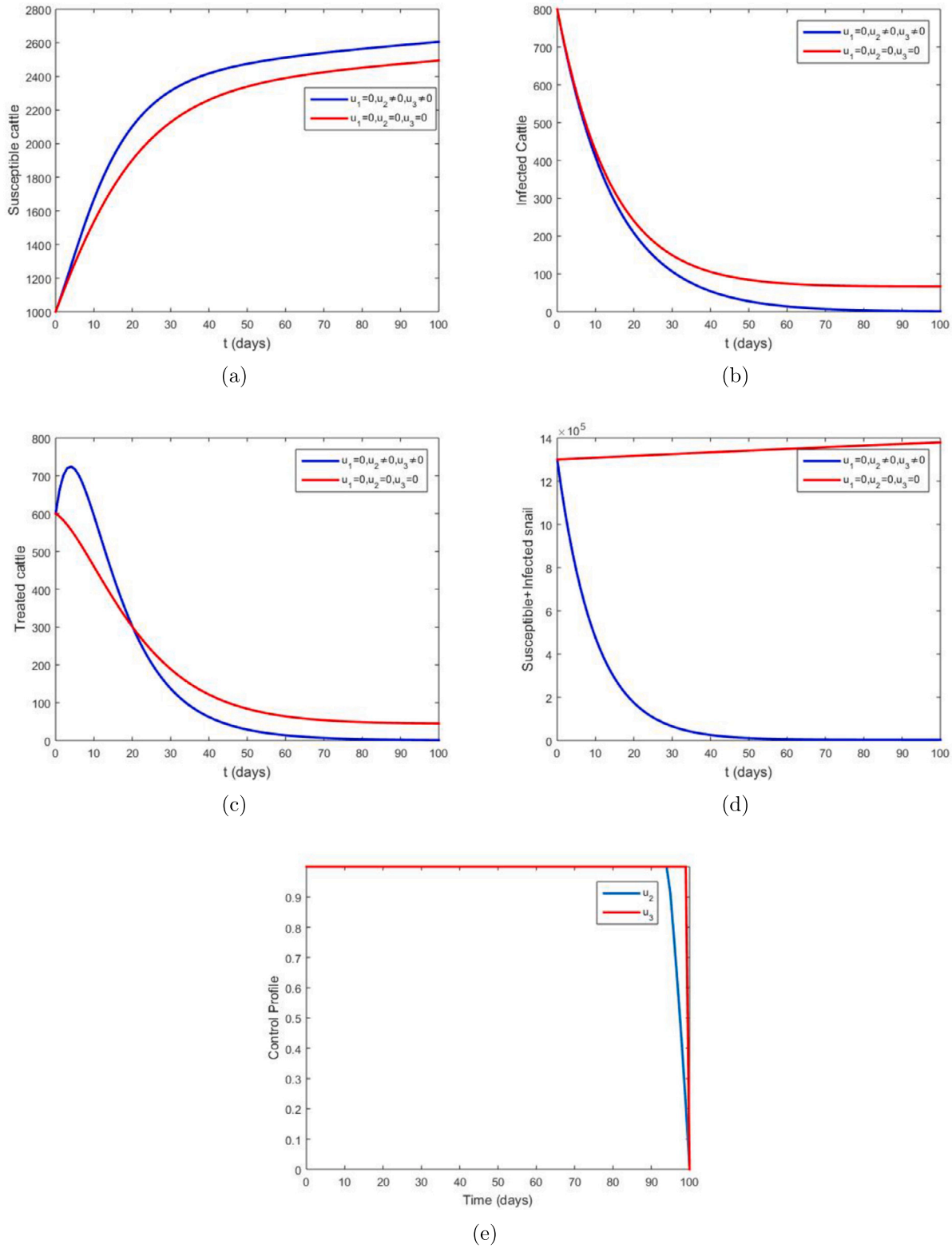

Fig. 6. The optimal combined effect of implementing cattle treatment ($u_2(t)$) and molluscicides ($u_3(t)$) for: (a) susceptible cattle, (b) infected cattle, (c) treated cattle, (d) total snail, and (e) control profile.

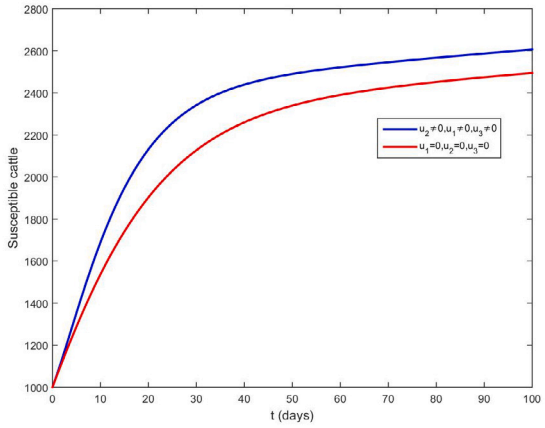

(a)

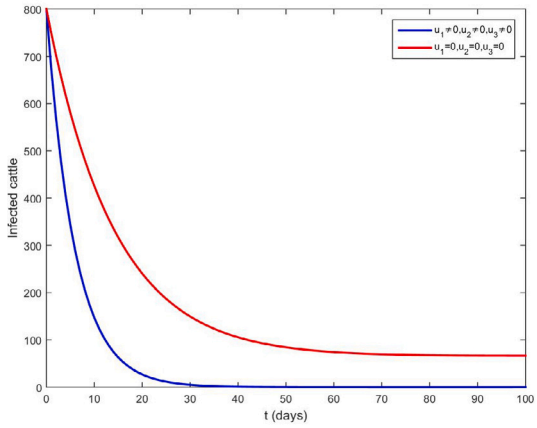

(b)

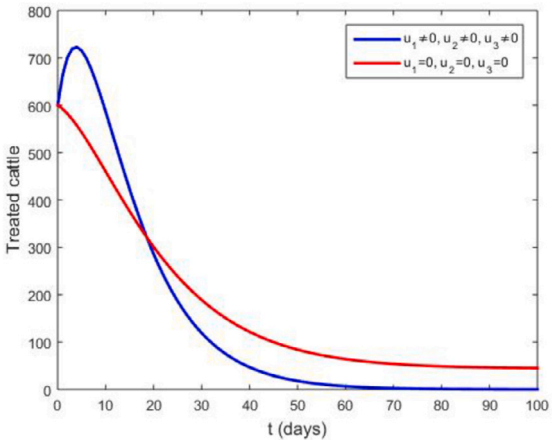

(c)

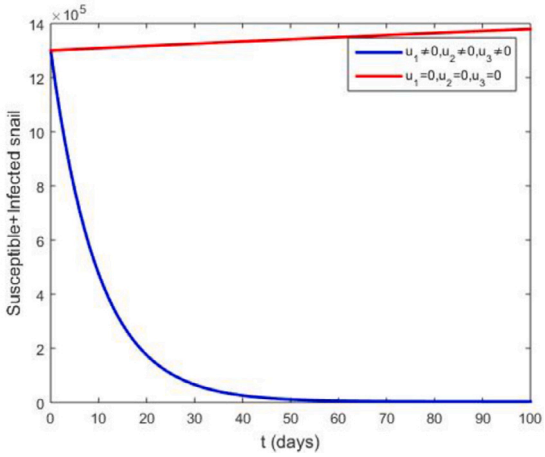

(d)

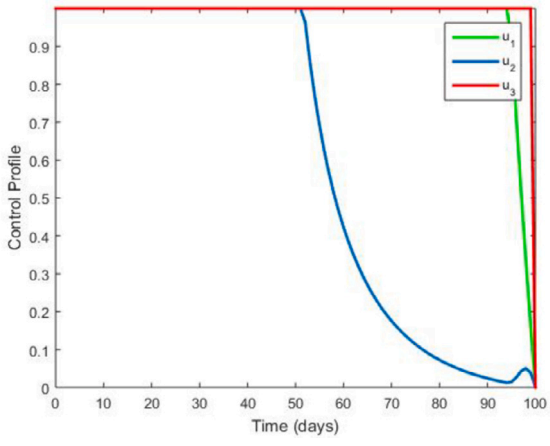

(e)

Fig. 7. The optimal combined effect of implementing pasture management ($u_1(t)$), cattle treatment ($u_2(t)$) and molluscicides ($u_3(t)$) for: (a) susceptible cattle, (b) infected cattle, (c) treated cattle, (d) total snail, and (e) control profile.

Table 3
Total amount of Fasciola hepatica infection averted and total cost for all strategies.

Strategies	Total infection averted	Total cost ($)
Strategy D (control u_1, u_2 and u_3)	5.1348×10^3	9.6074×10^5
Strategy A (control u_1 and u_2)	5.1369×10^3	6.2737×10^5
Strategy C (control u_2 and u_3)	5.6423×10^3	6.4329×10^5
Strategy B (control u_1 and u_3)	1.2289×10^4	7.1606×10^5

These results show that strategy B is more cost-effective and efficient than strategy C. Thus, Strategy B, including pasture management and molluscicides, becomes the best among the four strategies in that order, followed by strategies C, A, and D.

7. Conclusion

A mathematical model for an optimal control model for fasciola hepatica disease in cattle populations was formulated and analysed. The model provides a more profound comprehension of disease transmission and explores potential preventative and control approaches to slow disease progression. The endemic equilibrium of the model is globally asymptotically stable for $R_0 > 1$ and verified using the Volterra-Lyapunov approach. The sensitivity index of the Fasciola hepatica reproduction number to model parameters is calculated to assess the impact of each parameter. In the model, the most significant contributing parameter is the snail death rate, which indirectly affects the reproduction number of Fasciola hepatica.

The model considered three control measures in the optimum control problem: management of pastures, treatment of infected cattle, and the use of molluscicide. Necessary conditions for optimal control of the liver fluke disease are determined within the framework of Pontryagin's maximum principle. The numerical simulations for both double and triple-control strategies are carried out. All strategies under consideration turn out to be effective while reducing the infected cattle population. However, combined pasture management and treatment along with molluscicide significantly reduced the diseases in cattle, compared with double strategies. This result confirms the findings of Madubueze et al. [39].

Furthermore, it is shown in simulations that the value of the control parameter for the molluscicide intervention should always be at its maximum value for better control. This proves that molluscicide use plays a significant role in the control of fasciola hepatica, and this agrees with a previously done study by Nur et al. [50]. This is further supported by a study [51], which indicated that in areas where fascioliasis is endemic, the control of the population of the intermediate snail host is very promising in reducing transmission. Again, molluscicides against the snail hosts have also been a prospective tool in the control of fluke infection [52].

The cost-effectiveness analysis was done using the incremental cost-effectiveness ratio (ICER) to see the level of benefit and cost-effectiveness of these intervention strategies. The results indicate that combined pasture management and molluscicides were the most efficient and cost-effective strategies to eradicate Fasciola hepatic. The suggestions by the authors in [53] support the findings, where the use of different combinations of anthelmintics—probably by rotational strategies—will have better coverage against immature and adult flukes. We finally suggest that policymakers adopt a combined strategy involving pasture management and molluscicide intervention, as that will be the most cost-effective approach to controlling Fasciola hepatica disease.

CRediT authorship contribution statement

Dagnaw Tantie Yihunie: Writing – original draft, Software, Methodology, Investigation, Conceptualization. **Joseph Y.T. Mugisha:** Writing – review & editing, Validation, Supervision, Project administration, Investigation. **Dawit Melese Gebru:** Writing – review & editing, Visualization, Validation, Supervision, Software. **Haileyesus Tessema Alemneh:** Writing – review & editing, Visualization, Supervision, Methodology, Investigation, Conceptualization.

Declaration of competing interest

The authors declare that they have no known competing financial interests or personal relationships that could have appeared to influence the work reported in this paper.

Data availability

The research described in the article was conducted using secondary data from relevant published literature on the Fasciola hepatica Parameters and correspondingly cited.

References

[1] F. Borgsteede, Diseases of dairy animals–parasites, internal: liver flukes, 2011.
[2] C.M. Logue, N.L. Barbieri, D.W. Nielsen, Pathogens of food animals: sources, characteristics, human risk, and methods of detection, Adv. Food Nutr. Res. (2017) 277–365.
[3] S. Mas-Coma, V.H. Agramunt, M.A. Valero, Neurological and ocular fascioliasis in humans, Adv. Parasitol. 84 (2014) 27–149.

[4] N.C. Kamaruddin, M.A.I. Razali, I.E. Busayo, N.H. Hamzah, L.H. Idris, N.M. Md Isa, The first report of ruminant fascioliasis in Sabah, East Malaysia, J. Parasitol. Res. (2021) 6691483.
[5] R. Lalor, K. Cwiklinski, N.E.D. Calvani, A. Dorey, S. Hamon, J.L. Corrales, J.P. Dalton, C. De Marco Verissimo, Pathogenicity and virulence of the liver flukes fasciola hepatica and fasciola gigantica that cause the zoonosis fasciolosis, Virulence 12 (1) (2021) 2839–2867.
[6] M.D. Bargues, M.A. Valero, G.A. Trueba, M. Fornasini, A.F. Villavicencio, R. Guamán, D. Elías-Escribano, I. Pérez-Crespo, P. Artigas, S. Mas-Coma, et al., Dna multi-marker genotyping and cias morphometric phenotyping of fasciola gigantica-sized flukes from Ecuador, with an analysis of the radix absence in the new world and the evolutionary lymnaeid snail vector filter, Animals 11 (9) (2021) 2495.
[7] M. Diaby, O. Diop, E. Nassouri, A. Sène, M. Sène, Mathematical analysis of fasciola epidemic model with treatment and quarantine, in: International Workshop on Complex Systems Modelling & Simulation, Springer, 2019, pp. 133–149.
[8] A. Zewde, Y. Bayu, A. Wondimu, Prevalence of bovine fasciolosis and its economic loss due to liver condemnation at Wolaita sodo municipal abattair, Ethiopia, Vet. Med. Int. (2019) 9572373.
[9] K. Ashrafi, M.A. Valero, R.V. Peixoto, P. Artigas, M. Panova, S. Mas-Coma, Distribution of fasciola hepatica and f. gigantica in the endemic area of guilan, Iran: relationships between zonal overlap and phenotypic traits, Infect. Genet. Evol. 31 (2015) 95–109.
[10] D.D. Despommier, R.W. Gwadz, P.J. Hotez, Parasitic Diseases, Springer Science & Business Media, 2012.
[11] M.A. Caravedo, M.M. Cabada, Human fascioliasis: current epidemiological status and strategies for diagnosis, treatment, and control, Res. Rep. Trop. Med. 11 (2020) 149.
[12] W.J. Underwood, R. Blauwiekel, M.L. Delano, R. Gillesby, S.A. Mischler, A. Schoell, Biology and diseases of ruminants (sheep, goats, and cattle), in: Laboratory Animal Medicine, Elsevier, 2015, pp. 623–694.
[13] N. Che-Kamaruddin, N.F.S. Hamid, L.H. Idris, F.M. Yusuff, Z.H. Ashaari, H. Yahaya, N. Sahimin, N.M.M. Isa, Prevalence and risk factors of fasciolosis in a bovine population from farms in taiping, Malaysia, veterinary parasitology, Reg. Stud. Rep. 49 (2024) 100998.
[14] B. Alemu, Bovine fasciolosis in Ethiopia-a review, J. Vet. Anim. Res. 2 (2019) 202.
[15] U. Seid, M. Melese, Review on prevalence, distrbution and economic significance of liver fluke in Ethiopia, ARC J. Anim. Vet. Sci. (2018) 38–48.
[16] A. Wesolowska, K. Basalaj, L.J. Norbury, A. Sielicka, H. Wedrychowicz, A. Zawistowska-Deniziak, Vaccination against fasciola hepatica using cathepsin l3 and b3 proteases delivered alone or in combination, Vet. Parasitol. 250 (2018) 15–21.
[17] B. Admassu, A. Shite, G. Kinfe, A review on bovine fasciolosis, Eur. J. Biol. Sci. 7 (3) (2015) 139–146.
[18] M. Pan, S.-Y. Bai, T.-K. Ji, Y.-M. Fan, D.-D. Liu, Y. Yang, J.-P. Tao, S.-Y. Huang, Epidemiology of fasciola spp. in the intermediate host in China: a potential risk for fasciolosis transmission, Acta Trop. 230 (2022) 231–240.
[19] M. Ardo, Y. Aliyara, Prevalence of fasciolosis in small ruminants slaughtered at yola modern abattoir, adamawa state, Nigeria, Bayero J. Pure Appl. Sci. 7 (2) (2014) 13–16.
[20] X. García-López, L. Jaramillo-Meza, H. Quiroz-Romero, C. Arriaga-Díaz, J. Martínez-Maya, F. Diosdado-Vargas, F. Díaz-Otero, Effect of coinfection by fasciola hepatica and mycobacterium bovis on bovine tuberculosis immunodiagnosis in an enzootic area Hidalgo state, Mexico, J. Vet. Healthc. 1 (4) (2018) 41.
[21] L.G. Opio, E.M. Abdelfattah, J. Terry, S. Odongo, E. Okello, Prevalence of fascioliasis and associated economic losses in cattle slaughtered at lira municipality abattoir in northern Uganda, Animals 11 (3) (2021) 681.
[22] M. Barro, A. Guiro, D. Ouedraogo, Optimal control of a sir epidemic model with general incidence function and a time delays, CUBO 20 (02) (2018) 53–66.
[23] J. Turner, A. Howell, C. McCann, C. Caminade, R.G. Bowers, D. Williams, M. Baylis, A model to assess the efficacy of vaccines for control of liver fluke infection, Sci. Rep. (2016) 1–13.
[24] Z. Avazzadeh, H. Hassani, P. Agarwal, S. Mehrabi, M. Javad Ebadi, M.K. Hosseini Asl, Optimal study on fractional fascioliasis disease model based on generalized Fibonacci polynomials, Math. Methods Appl. Sci. 46 (8) (2023) 9332–9350.
[25] O.M. Ogunmiloro, Mathematical analysis and approximate solution of a fractional order Caputo fascioliasis disease model, Chaos Solitons Fractals 146 (2021) 110851.
[26] T.M. León, T.C. Porco, C.S. Kim, S. Kaewkes, W. Kaewkes, B. Sripa, R.C. Spear, Modeling liver fluke transmission in northeast Thailand: impacts of development, hydrology, and control, Acta Trop. 188 (2018) 101–107.
[27] E. Goodall, S. McIlroy, R. McCracken, E. McLoughlin, S. Taylor, A mathematical forecasting model for the annual prevalence of fasciolosis, Agric. Syst. 36 (2) (1991) 231–240.
[28] O.M. Ogunmiloro, Optimal control analysis of fascioliasis disease transmission dynamics, Appl. Math. 50 (2) (2022).
[29] E. Kanyi, A.S. Afolabi, N.O. Onyango, Mathematical modeling and analysis of transmission dynamics and control of schistosomiasis, J. Appl. Math. (2021) 6653796.
[30] E.T. Chiyaka, W. GARIRA, Mathematical analysis of the transmission dynamics of schistosomiasis in the human-snail hosts, J. Biol. Syst. 17 (03) (2009) 397–423.
[31] J.K.K. Asamoah, B. Safianu, E. Afrifa, B. Obeng, B. Seidu, F.A. Wireko, G.-Q. Sun, Optimal control dynamics of gonorrhea in a structured population, Heliyon 9 (10) (2023).
[32] P. van den Driessche, J. Watmough, Reproduction numbers and sub-threshold endemic equilibria for compartmental models of disease transmission, Math. Biosci. 180 (1–2) (2002) 29–48.
[33] J.K.K. Asamoah, Z. Jin, G.-Q. Sun, Non-seasonal and seasonal relapse model for q fever disease with comprehensive cost-effectiveness analysis, Results Phys. 22 (2021) 103889.
[34] C. Chavez, Z. Feng, W. Huang, On the computation of r_0 and its role on global stability, mathematical Approaches for Emerging and Re-emerging Infection Diseases: an introduction 125 (2002) 31–65.
[35] M.S. Zahedi, N.S. Kargar, The Volterra–Lyapunov matrix theory for global stability analysis of a model of the hiv/aids, Int. J. Biomath. 10 (01) (2017) 1750002.
[36] M. Masoumnezhad, M. Rajabi, A. Chapnevis, A. Dorofeev, S. Shateyi, N.S. Kargar, H.S. Nik, An approach for the global stability of mathematical model of an infectious disease, Symmetry 12 (11) (2020) 1778.
[37] F. Chien, S. Shateyi, Volterra–Lyapunov stability analysis of the solutions of babesiosis disease model, Symmetry 13 (7) (2021) 1272.
[38] Z. Sun, A time-varying matrix solution to the Brockett decentralized stabilization problem, arXiv preprint, arXiv:2303.15924, 2023.
[39] C.E. Madubueze, R.I. Gweryina, A. Abokwara, Mathematical analysis and optimal control of schistosomiasis transmission model, Biomath Commun. 9 (1) (2022) 2203071.
[40] M. Zamir, G. Zaman, A.S. Alshomrani, Sensitivity analysis and optimal control of anthroponotic cutaneous leishmania, PLoS ONE 11 (8) (2016) e0160513.
[41] A. Bat, A. Kamil, et al., Optimal control of a production inventory system with generalized Pareto distributed deterioration items, J. Appl. Sci. 10 (2) (2010) 116–123.
[42] J.K.K. Asamoah, Z. Jin, G.-Q. Sun, B. Seidu, E. Yankson, A. Abidemi, F. Oduro, S.E. Moore, E. Okyere, Sensitivity assessment and optimal economic evaluation of a new covid-19 compartmental epidemic model with control interventions, Chaos Solitons Fractals 146 (2021) 110885.
[43] P.M. Mwamtobe, S. Abelman, J.M. Tchuenche, A. Kasambara, et al., Optimal (Control of) Intervention Strategies for Malaria Epidemic in Karonga District, Malawi, Abstract and Applied Analysis, vol. 2014, Hindawi, 2015.
[44] L.S. Pontryagin, Mathematical Theory of Optimal Processes, Routledge, 2018.
[45] J.K.K. Asamoah, E. Okyere, A. Abidemi, S.E. Moore, G.-Q. Sun, Z. Jin, E. Acheampong, J.F. Gordon, Optimal control and comprehensive cost-effectiveness analysis for covid-19, Results Phys. 33 (2022) 105177.
[46] G. Rahmann, H. Seip, Alternative strategies to prevent and control endoparasite diseases in organic sheep and goat farming systems–a review of current scientific knowledge, Ressortforschung für den Ökologischen Landbau 2006 (2006) 49–90.

[47] G. Knubben-Schweizer, S. Rüegg, P.R. Torgerson, C. Rapsch, F. Grimm, M. Hässig, P. Deplazes, U. Braun, Control of bovine fasciolosis in dairy cattle in Switzerland with emphasis on pasture management, Vet. J. 186 (2) (2010) 188–191.
[48] J.K.K. Asamoah, E. Yankson, E. Okyere, G.-Q. Sun, Z. Jin, R. Jan, et al., Optimal control and cost-effectiveness analysis for Dengue fever model with asymptomatic and partial immune individuals, Results Phys. 31 (2021) 104919.
[49] A. Kouidere, O. Balatif, M. Rachik, Cost-effectiveness of a mathematical modeling with optimal control approach of spread of covid-19 pandemic: a case study in Peru, Chaos Solitons Fractals X 10 (2023) 100090.
[50] W. Nur, T. Trisilowati, A. Suryanto, W.M. Kusumawinahyu, Optimal Control Problem and Cost-Effectiveness Analysis of Schistosomiasis Model, AIP Conference Proceedings, vol. 2498, AIP Publishing, 2022.
[51] T. Solomon, B. Alemu, Economic loss caused by organ condemnation in cattle slaughtered at hawassa municipal abattoir, southern Ethiopia, J. Glob. Biosci. 8 (2) (2019) 5966–5977.
[52] F. TT, Review on epidemiology, control and public health importance of bovine fasciolosis, Austin J. Vet. Sci. Anim. Husbandry 8 (2) (2021) 1082.
[53] H.M. Rizwan, M.S. Sajid, H. Abbas, S. Ghazanfer, M. Arshad, An insight into different strategies for control and prophylaxis of fasciolosis: a review, J. Adv. Int. Vet. Res. 4 (1) (2022) 5–14.